

# Mapping the bound conformation and protein interactions of microtubule destabilizing peptides by STD–NMR spectroscopy

Mark J. Milton,<sup>†</sup> R. Thomas Williamson<sup>‡</sup> and Frank E. Koehn\*

Wyeth Research, Chemical and Screening Sciences, 401 North Middletown Road, Pearl River, NY 10965, USA

Received 6 April 2006; revised 18 May 2006; accepted 18 May 2006  
Available online 12 June 2006

**Abstract**—Using the hemiasterlin analogs taltobulin (**I**, HTI-286), **II**, and **III** as model compounds, we demonstrate that relaxation-compensated STD–NMR can be used as an effective tool to efficiently provide a qualitative epitope map for microtubule destabilizing peptides. Due to the disparate relaxation behavior of the protons in these model compounds, it was essential to collect STD with very short saturation times to render an accurate picture of the binding interaction. The conformation of HTI-286 (**I**) in complex with the protein was determined from TRNOESY/ROESY experiments and is similar to the X-ray crystal structure conformation observed for hemiasterlin methyl ester in the absence of protein.

© 2006 Elsevier Ltd. All rights reserved.

Several natural products with antimitotic activity are currently being evaluated in clinical trials as anticancer agents. Generally, these compounds can be classified as either microtubule stabilizing agents such as Taxol® and its analogs or microtubule destabilizing agents like the Vinca alkaloids.<sup>1</sup> Additional antimitotic compounds are in preclinical development or clinical trials.<sup>2</sup> Taltobulin (**I**, HTI-286), an analog of the marine natural product hemiasterlin,<sup>3</sup> is a potent inhibitor of microtubule formation that has progressed to Phase II clinical trial for the treatment of cancer.<sup>4</sup> Knowledge is increasing of how HTI-286 and its derivatives inhibit microtubule formation at the molecular level.<sup>5,11</sup> However, additional characterization of the  $\alpha/\beta$ -tubulin–HTI-286 interaction may aid further in the development of inhibitors that show more potent activity or improved physical properties.

NMR spectroscopy has been used extensively for probing protein–ligand interactions. Recently, the saturation-transfer-difference (STD) method has enjoyed a resurgence in the literature.<sup>6</sup> STD experiments rely on

the transfer of magnetization from a protein, which has been irradiated for several seconds, to a rapidly exchanging ligand. Protons from the ligand that have the closest association with the protein surface, and therefore contribute strongly to the binding interaction, should experience the largest amount of magnetization transfer and in turn the largest signal enhancements. In theory, STD experiments result in 1D spectra whose signal intensity is modulated by the proton's proximity to the protein in the complex.

Figure 1 shows the structure of HTI-286 (**I**) and Table 1 lists the STD percentage enhancements for 1 s of saturation. The STD enhancements measured at 1 s saturation suggest that the aromatic group makes the closest association with the protein, whereas, the *tert*-butyl (H10),

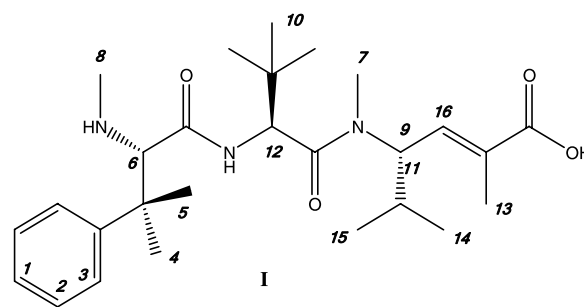


**Figure 1.** Structure of HTI-286 (**I**) showing proton numbering convention used in this text.

**Keywords:** Hemiasterlin; Saturation transfer difference; TRNOESY; STD–NMR; Taltobulin; HTI-286; Tubulin; Tubulin binding; Microtubule destabilization.

\* Corresponding author. Tel.: +1 845 602 4094; fax: +1 845 602 6005; e-mail: [koehnf@wyeth.com](mailto:koehnf@wyeth.com)

<sup>†</sup> Present address: Millenium Pharmaceuticals, Cambridge, MA, USA.

<sup>‡</sup> Present address: Roche Pharmaceuticals, Florence, SC, USA.

**Table 1.** Absolute and relative STD transfers for HTI-286-tubulin complex at two saturation frequencies

Saturation time	proton number	Proton type	1 s		0.35 s		$T_{\text{(sel)}}$
			Absolute (%)	Relative (%)	Absolute (%)	Relative (%)	
2		Aro	1.52	67	0.59	77	
3		Aro	1.74	77	0.66	87	
1		Aro	2.09	100	0.77	100	650
16		DB	1.29	50	0.53	69	
9		Alpha	1.45	69	0.66	40	540
12		Alpha	1.70	61	0.34	78	
6		Alpha	2.30	58	0.63	47	
7		N-CH <sub>3</sub>	0.78	49	0.39	51	
8		N-CH <sub>3</sub>	0.78	38	0.35	46	735
13		C-CH <sub>3</sub>	0.94	50	0.38	50	
4		CH <sub>3</sub> × 2	0.41	21	0.29	38	
5		CH <sub>3</sub> × 2	0.45	21	0.30	39	
10		CH <sub>3</sub> × 3	0.29	16	0.17	22	360
14		CH <sub>3</sub> × 2	0.79	24	0.41	53	
15		CH <sub>3</sub> × 2	0.69	31	0.36	47	

Proton type: Aro, aromatic; DB, double bond; Alpha, alpha type p; R-CH<sub>3</sub>, isolated methyl group; CH<sub>3</sub> × 2, *gem*-dimethyl group; CH<sub>3</sub> × 3, *tert*-butyl group.

valine (H14/15), and H4/5 geminal methyl protons have a significantly diminished interaction with the protein. It is known from SAR studies that branching at the *tert*-butyl correlates with potency of tubulin inhibition,<sup>7</sup> a finding consistent with the 1 s STD measurements. However, these same studies demonstrate that the aromatic group of **1** can tolerate significant structural changes while retaining good inhibition of tubulin polymerization, and that larger groups at H14/15 and H4/5 lead to less potent analogs.<sup>5,7</sup> Indeed, SAR studies show that the H4/5 *gem*-dimethyl is a key component necessary for potent activity. This does not correlate with the 1 s STD results. Furthermore, the 1 s STD enhancements observed for the H13 and H16 protons suggest a closer interaction than that for H4/5. The SAR, however, shows the role of the olefin to be more important for conformational rigidity than for close contact of its substituents.<sup>7</sup>

The discrepancies described above prompted us to examine the STD results more closely. At 1 s irradiation time, the extent of STD transfer was highly dependent on the type of proton in the molecule (see Table 1), that is, the extent of saturation transfer occurs in the following order: aromatic protons > alpha protons > non-coupled methyl groups > coupled methyl groups. Yan and co-workers<sup>8</sup> have observed that aromatic protons behave differently than methyl protons in STD experiments, and suggest reducing the saturation time in order to compensate for the large difference in  $T_2$  times between the two groups.

To fully account for the effects of relaxation, STD data were acquired on **1** complexed with tubulin at a series of saturation times (Fig. 2). As shown in Figure 2, the signal enhancement for the methyl protons (H10, H4/5, and H14/15) reaches a plateau after just a few hundred milliseconds of irradiation. Conversely, the aromatic and alpha protons (H6, H12, and H9) continue to show a build-up even to a 2 s saturation time. These STD build-ups correlate well with the  $T_{1\text{ selective}}$  data (Table 1) for the representative protons.<sup>12</sup>

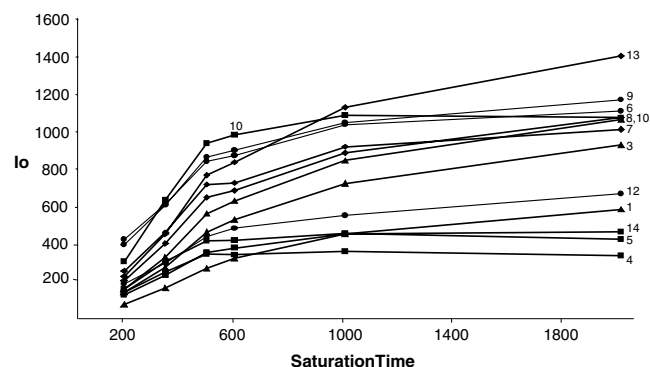


**Figure 2.** STD buildup profile, intensity ( $I_0$ ) versus saturation time (ms) for 200:1 HTI-286:tubulin system. —■— coupled methyl; —●— alpha; —◆— isolated methyl; —▲— aromatic protons. Proton numbers (see Fig. 1) listed on right.

The build-up curves show that rapidly relaxing groups, such as the *tert*-butyl group, will be underrepresented and that slowly relaxing protons such as aromatics will be overrepresented in STD experiments with long saturation times. It would be expected that the best STD transfer data should come from experiments acquired at very short saturation times, where all protons exhibit similar behavior. Indeed, the data collected at 350 ms display markedly less demarcation according to proton type (Table 1); however, the experiments required hours rather than minutes of acquisition in order to build up sufficient signal intensity for data analysis. When measured with a 350 ms irradiation, the relaxation-compensated STD values show the aromatic group forming a close interaction with the protein, and the *tert*-butyl group being not in close association with the protein. These data are consistent with SAR observations that large pendant groups (see Fig. 3) may be attached in place of *tert*-butyl without significant loss in affinity or activity.<sup>7</sup> Importantly the relaxation-compensated STD data show stronger protein contact for H4/5, C8, H14/15, H16 and weaker interaction for H6 and H9.

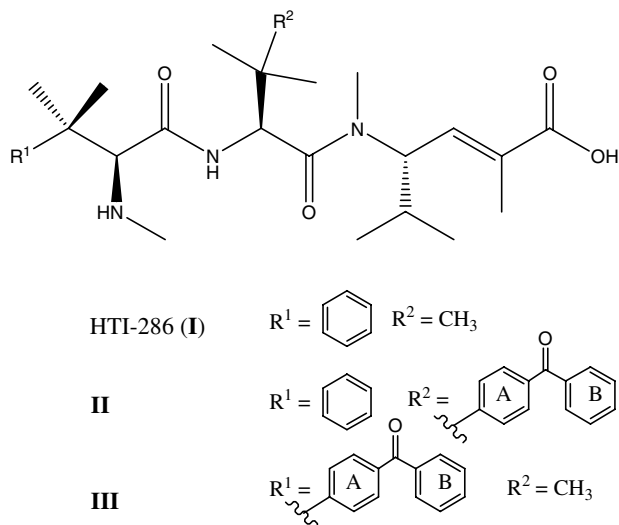


Figure 3. HTI-286 and analogs.

Additional STD experiments were performed on tubulin complexes of HTI-286 analogs **II** and **III** to probe the binding interaction. (Fig. 3) **II** and **III** were chosen because they have been used extensively in photoaffinity labeling and iterative docking studies and bear substituents that extend several Angstroms from the parent structure. Yet, each retains good tubulin binding activity.<sup>9,11</sup> In **II**, the *tert*-butyl group is extended by addition of a benzophenone group and in **III** the phenyl group of HTI-286 is extended with the addition of a *p*-benzoyl group. Data measured with a saturation time of 350 ms on samples containing a 200-fold excess of these analogs to tubulin showed high STD transfers to the protons of both phenyl rings. In fact, in **II** STD transfer to the distal ring B is higher than that for proximal Ring A. (Table 2). These observations initially seemed inconsistent with the low (22%) STD transfer measured for the *tert*-butyl group in **I** (Table 1), and suggest that relaxation effects may still be a problem in this system. However, they may also indicate that the *tert*-butyl group of **I** occupies a spacious cavity. In **II** the benzophenone group extends to fill the void and as a result makes closer contact with the protein. The magnitude of STD transfer suggests that the distal aromatic ring in **II** may be  $\pi$ -stacking with an aromatic side chain. This would explain why the UV-sensitive benzophenone

Table 2. STD transfer at 350 ms saturation time for HTI-286 (**I**) and analogs **II** and **III**, numbering system same as for HTI-286: well-resolved protons from the aromatic substituent groups were analyzed for STD transfer

	Proton number	STD (%)
HTI-286 ( <b>I</b> )	3	77
	2	87
	1	100
<b>II</b>	Ring A	89
	Ring B	113
<b>III</b>	Ring A	100
	Ring B	85

Ring A and B listed in Figure 3.

group of **II** is both photoreactive with  $\alpha$ -tubulin and retains good binding activity.<sup>9</sup> The extended aromatic moiety of **III** shows very efficient conductivity of magnetization (85%), suggesting that it retains good contact with the protein surface. This correlates with the fact that **III** is a good photoprobe.<sup>9</sup>

Transferred NOESY data (data not shown) were recorded and used to calculate the bound conformation of **I** when complexed to tubulin.<sup>12</sup> Four inter-residue TRNOE's between side-chain methyls were observed and these were used to describe the global fold of the tripeptide (TRNOESY peaks which arise as a result of spin diffusion were identified by acquiring TRROESY data sets). TRNOE's were observed between only one of two valine methyls (H14/15) and the H4 and H5 methyl groups. These NOE's were also observed in the absence of protein indicating that this methyl–methyl interaction helps stabilize the formation of the biologically active fold. TRNOESY correlations used in a restrained simulated annealing protocol are shown in Figure 4. This produced a family of structures of which the lowest energy conformation is displayed (Fig. 4).

The NMR derived structure for tubulin-bound **I** resembles the X-ray crystal structure solved for hemiasterlin methyl ester in the absence of protein,<sup>10</sup> with the exception that the phenyl group of **I** is rotated about its bonding axis to the backbone by 60° compared to the indole of hemiasterlin methyl ester (Fig. 4). The barrier to rotation about this bond is expected to be small. The *tert*-butyl (H10), methylamine (H8), and *N*-methyl (H7) groups are super-imposable. The NMR structure of protein-

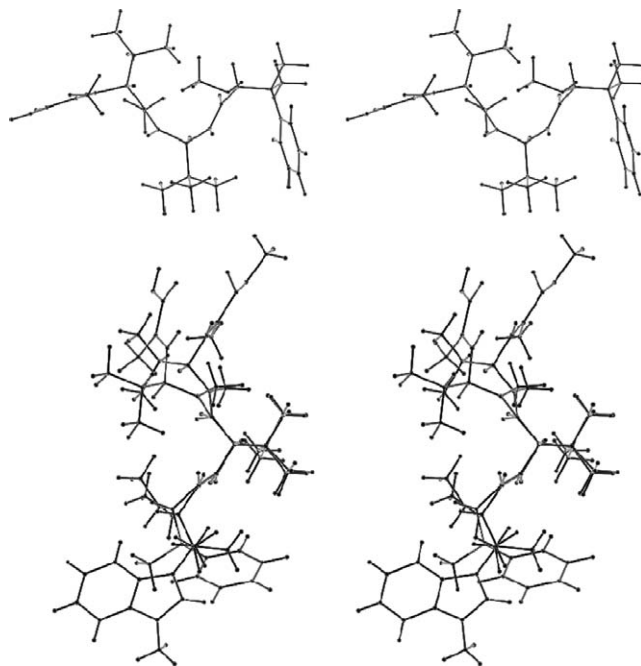


Figure 4. (Top) Stereo view of the bound conformation of HTI-286 derived from TRNOESY data coupled with restrained simulated annealing. The following restraints were applied during the annealing: C15-C4; C15-C5; C15-C8; C15-C7; C15-H12 and C14-H13. (Bottom) Superimposition of the NMR derived structure of HTI-286 with the X-ray crystal structure of hemiasterlin methyl ester.<sup>9</sup>

bound **I** is more folded than the X-ray structure of hemiasterlin methyl ester. This tightening of the fold is required so the observed NOE's between H15 and H4/5 can be back calculated from the model. The NMR structure of tubulin-bound **I** derived by TRNOESY is similar to that obtained by Ravi et al. via iterative docking, particularly with regard to the relative orientation of the H4/5, H10, and H14/15.<sup>11</sup>

Relaxation-compensated STD–NMR experiments and TRNOESY/ROESY experiments have been used to investigate the binding interaction and bound conformation of the antimitotic agent HTI-286 in complex with tubulin. When measured under short irradiation time to minimize relaxation effects, the STD data show that the aromatic group of HTI-286 interacts strongest with protein. The side-chain protons H4/5, C8, H14/15, and H16 also interact strongly. The *tert*-butyl (H10) shows minimal interaction by NMR. These results agree well with the binding model developed by Ravi et al. using iterative docking experiments, photoaffinity labeling, and structure–activity relationships.<sup>11</sup> In this model, the HTI-286 molecule is bound in a pocket on the  $\beta$  subunit, proximal to the interdimer interface, with the phenyl ring  $\pi$ -stacked against the aromatic side chain of Phe351 of  $\alpha$ -tubulin. The *tert*-butyl group occupies a spacious cavity in  $\beta$ -tubulin, oriented toward the protein surface but not making close contact with it.

TRNOESY/ROESY experiments also show that the bound and unbound conformations of HTI-286 are similar with regard to the relative orientation of the *gem*-dimethyl, and valine side chain, features seen in the X-ray structure of hemiasterlin methyl ester as well. Selection by tubulin of solution conformers of **I** may contribute to favorable thermodynamics of binding and care should be exercised in analog design so as not to disrupt this solution conformation. Finally, the HTI-286-tubulin system provides a strong example of the deleterious effects of differential proton relaxation on STD measurements, and could serve as a useful model system for the development of methods to compensate for the affects of relaxation in STD experiments.

### Acknowledgments

We thank Arie Zask, Girija Krishnamurthy, and Malaithi Hari of Wyeth Research for helpful discussions, and for supplies of HTI-286 and analogs. We also particularly thank Malini Ravi for insights into the molecular modeling study.

### References and notes

- Jordan, M. A.; Wilson, L. *Nat. Rev. Can.* **2004**, *4*, 253.

- (a) Cohen, P. *Nat. Rev. Drug Disc.* **2002**, *1*, 309; (b) Blume-Jensen, P.; Hunter, T. *Nature* **2001**, *411*, 355.
- (a) Talpir, R.; Benayahu, Y.; Kashman, Y.; Pannell, L.; Schleyer, M. *Tetrahedron Lett.* **1994**, *35*, 4453; (b) Anderson, H. J.; Coleman, J. E.; Anderson, R. J.; Roberge, M. *Cancer Chemother. Pharmacol.* **1997**, *39*, 223.
- Ratain, M. J.; Undevia, S.; Janisch, I.; Roman, S.; Mayer, P.; Buckwalter, M.; Foss, D.; Hamilton, B. L.; Fisscher, J.; Bukowski, R. M. *Proc. Am. Soc. Clin. Oncol.* **2003**, *22*, 129.
- Lo, M.-C.; Aulabaugh, A.; Krishnamurthy, G.; Kaplan, J.; Zask, A.; Smith, R.; Ellestad, G. *J. Am. Chem. Soc.* **2004**, *126*, 9898.
- (a) Mayer, M.; Meyer, B. *J. Am. Chem. Soc.* **2001**, *123*, 6108; (b) Meyer, B.; Peters, T. *Angew. Chem., Int. Ed.* **2003**, *42*, 890; (c) Herfurth, L.; Ernst, B.; Wagner, B.; Ricklin, D.; Strasser, D. S.; Magnani, J. L.; Benie, A. J.; Peters, T. *J. Med. Chem.* **2005**, *48*, 6879; (d) Soubias, O.; Gawrisch, K. *J. Am. Chem. Soc.* **2005**, *127*, 13110.
- Zask, A.; Birnberg, G.; Cheung, K.; Kaplan, J.; Niu, C.; Norton, E.; Suayan, R.; Yamashita, A.; Cole, D.; Tang, Z.; Krishnamurthy, G.; Williamson, R. T.; Khafizova, G.; Musto, S.; Hernandez, R.; Annable, T.; Yang, X.; Discafani, C.; Beyer, C.; Greenberger, L.; Loganzo, F.; Ayral-Kaloustian, S. *J. Med. Chem.* **2004**, *47*, 4774.
- Yan, J. et al. *J. Magn. Res.* **2003**, *163*, 270.
- Nunes, M.; Kaplan, J.; Wooters, J.; Hari, M.; Minnick, A. A.; May, M. K.; Shi, C.; Musto, S.; Beyer, C.; Krishnamurthy, G.; Qui, Y.; Loganzo, F.; Ayral-Kaloustian, S.; Zask, A.; Greenberger, L. M. *Biochemistry* **2005**, *44*, 6844.
- Coleman, J. E.; Patrick, B. O.; Andersen, R. J.; Rettig, S. J. *Acta Crystallogr. Sect., C* **1996**, *C52*, 1525.
- Ravi, M.; Zask, A.; Rush, T. S. *Biochemistry* **2005**, *44*, 15871.
- Experimental details*—NMR data were collected at 400 MHz and samples were equilibrated at 310 K. For STD–NMR: 200:1 ligand to tubulin (20  $\mu$ M) samples were prepared in deuterated  $K_2PO_4$  buffer, pD 7.0. STD data were acquired over a range of protein saturation time (0.2–5 s). Saturation pulses consisted of 50 ms Gaussian trains centered on 4.55 and 0.00 ppm. STD transfer figures were taken from a weighted average of both saturation frequencies. All STD experiments featured a short  $T1\rho$  filter to reduce protein signal. A 200-fold excess of sucrose was added to a sample to confirm that STD signals were specific.  $T1$  selective values were obtained from a modified  $T1$  experiment in which the second  $180^\circ$  pulse is replaced with a selective pulse. 1D selective-TRNOESY/ROESY experiments were performed on 240:1 ligand to tubulin sample. 2K scans per experiment with an R/NOE mixing time of 200 ms. 1D selective NOESY data collected for the ligand in the absence of protein were performed with a 500 ms mixing time. Molecular modeling was performed using InsightII/Discover-3 (Accelrys) software. Restraints were applied as a square-well potential function; the upper limit of the function was set at 6 Å. The X-ray structure of hemiasterlin was modified and used in a pseudorandomization protocol (300 ps dynamics at 1000 K) then the structure was subjected to restrained simulated annealing to 10 K then minimized and saved. A total of 10 structures were generated to cover the conformational space.